TP53/p53 Facilitates Stress-Induced Exosome and Protein Secretion by Adipocytes

Yimao Huang,[1] Ann V. Hertzel,[1] Shayla R. Fish,[1] Catherine L. Halley,[1] Ellie K. Bohm,[1] Hector Martell Martinez,[1,2] Cameron C. Durfee,[1] Mark A. Sanders,[3] Reuben S. Harris,[1] Laura J. Niedernhofer,[1,2] and David A. Bernlohr[1,2,4]

Diabetes 2023;72:1560–1573 | https://doi.org/10.2337/db22-1027

Besides the secretion of fatty acids, lipolytic stimulation of adipocytes results in the secretion of triglyceride-rich extracellular vesicles and some free proteins (e.g., fatty acid binding protein 4) that, in sum, affect adipose homeostasis as well as the development of metabolic disease. At the mechanistic level, lipolytic signals activate p53 in an adipose triglyceride lipase–dependent manner, and pharmacologic inhibition of p53 attenuates adipocyte-derived extracellular vesicle (AdEV) protein and FABP4 secretion. Mass spectrometry analyses of the lipolytic secretome identified proteins involved in glucose and fatty acid metabolism, translation, chaperone activities, and redox control. Consistent with a role for p53 in adipocyte protein secretion, activation of p53 by the MDM2 antagonist nutlin potentiated AdEV particles and non-AdEV protein secretion from cultured 3T3-L1 or OP9 adipocytes while the levels of FABP4 and AdEV proteins were significantly reduced in serum from p53$^{-/-}$ mice compared with wild-type controls. The genotoxin doxorubicin increased AdEV protein and FABP4 secretion in a p53-dependent manner and DNA repair–depleted ERCC1$^{-/\Delta}$–haploinsufficient mice expressed elevated p53 in adipose depots, along with significantly increased serum FABP4. In sum, these data suggest that lipolytic signals, and cellular stressors such as DNA damage, facilitate AdEV protein and FABP4 secretion by adipocytes in a p53-dependent manner.

ARTICLE HIGHLIGHTS

- This study was undertaken to discover mechanism(s) leading to regulated protein secretion by adipocytes.
- We tested the hypothesis that TP53/p53 is required for regulated protein secretion.
- Our studies identified that TP53/p53 is required for protein secretion and is regulated by several stress inducers, such as nutrient deprivation and/or DNA damage.
- These studies may provide a mechanistic link among TP53/p53 mutations, cancer, and obesity.

Adipose tissue serves as a central node in energy metabolism and regulates whole-body homeostasis (1,2). Mechanistically, adipose tissue functions as an endocrine organ and secretes many adipokines, lipokines, and hormones in response to varying physiological conditions and metabolic disorders (3). Indeed, different secretomes can be produced by adipocytes responding to physiological stimuli such as nutrient abundance, nutrient deprivation, or inflammation (4).

Adipocyte-derived extracellular vesicles (AdEVs) are small extracellular vesicles with a diameter of 50–150 nm that contain a variety of cargo, including proteins, lipids, mRNA, organelles, and miRNA, that can serve as intercellular and interorgan communication vehicles (5,6). Adipocytes release vesicles depending on changes in the metabolic state(s) of the organism. For example, obesity results in increased vesicle secretion specifically from adipocytes, and not from other cell types in adipose tissue (7). Characterization of the secreted AdEVs have revealed two subtypes of vesicles, small and large, with overlapping but also unique associated proteins (8).

[1]Department of Biochemistry, Molecular Biology and Biophysics, University of Minnesota, Minneapolis, MN
[2]Institute on the Biology of Aging and Metabolism, University of Minnesota, Minneapolis, MN
[3]University Imaging Center, University of Minnesota, Minneapolis, MN
[4]Institute for Diabetes, Obesity and Metabolism, University of Minnesota, Minneapolis, MN

Corresponding author: David A. Bernlohr, Bernl001@umn.edu

Received 15 December 2022 and accepted 6 June 2023

This article contains supplementary material online at https://doi.org/10.2337/figshare.23553357.

Y.H. and A.V.H. share first authorship.

See accompanying article, p. 1521.

Adipocyte extracellular vesicles are triglyceride rich such that they stay suspended upon ultracentrifugation (9).

Released AdEVs play an active role in communication between cells within adipose, including immune and endothelial cells, as well as to signal more distant cells or organs. More specifically, AdEVs have been demonstrated to increase M1 macrophages, resulting in enhanced inflammation and insulin resistance. Additionally, recent studies have shown that mitochondrial stress stimulates release of a population of adipocyte-derived vesicles that contain damaged mitochondria (10,11). These AdEVs induced oxidative stress in cardiomyocytes and, through hormesis, protect the heart from additional ischemic injury (12). In response to lipolysis, a pathway that is increased with obesity-induced insulin resistance, adipocytes secrete proteins that lack a classic secretion signal and thus use a mechanism distinct from the conventional endoplasmic reticulum–Golgi secretory system (13,14), including such proteins as nicotinamide phosphoribosyl transferase, FABP4, and FABP5 (15,16). This secretion is dependent on adipose triglyceride lipase (ATGL), sirtuin 1, and monounsaturated fatty acids, and require some, but not all, autophagic components (16). Secreted forms of FABP4 and FABP5 are not associated to any extent with the secreted AdEVs. FABP4 belongs to a multigene family of fatty acid–binding proteins that function in lipid trafficking and intracellularly signaling (17,18). FABP4-null mice are protected from obesity-dependent metabolic dysfunction such as type 2 diabetes, asthma, inflammation, and certain types of cancers (17,19–21).

Herein, we provide findings demonstrating that in adipocytes, p53 facilitates AdEV and protein secretion in response to nutrient restriction–associated lipolytic stimuli and/or DNA damage.

RESEARCH DESIGN AND METHODS

Reagents and Chemicals

Forskolin (FSK; catalog no. 66575-29-9), ATGListatin (hereafter, ASTAT) (catalog no. SML1075), 8-bromo-cAMP (8-Br-cAMP; catalog no. B7880), and Iso (catalog no. 51-30-9) were purchased from Sigma-Aldrich. Torin1 (catalog no. S2827), rapamycin (catalog no. S1039), nutlin (catalog no. S8059), and doxorubicin (DOXO; catalog no. S1208) were purchased from Selleckchem.

Animal Studies

TP53-null animals were obtained from Jackson Laboratory (mouse stock no. 002101) and housed in specific pathogen-free animal-care facilities at the University of Minnesota Twin Cities. All experiments were approved by and performed in accordance with the relevant guidelines and regulations from the University of Minnesota Institutional Animal Care and Use Committee (protocol 2201-39748A).

Cell Culture and Differentiation

3T3-L1 cells were maintained as fibroblastic preadipocytes and differentiated to mature adipocytes as described previously (16). OP9 preadipocytes were grown and maintained in α-minimum essential medium (α-MEM) with 20% FBS and differentiated with α-MEM containing 0.2% FBS, 175 nmol/L insulin, 900 μmol/L oleate bound to albumin (4:1 oleate to albumin) for 48 h. Differentiated OP9 cells were maintained in α-MEM containing 0.2% FBS until used.

To generate p53-silenced 3T3-L1 cells, 3T3-L1 cells were transduced with a pLKO.1-based shRNA lentivirus for p53 (sense, CGCGCCATGGCCATCTACA) using a recombinant lentivirus packaged from HEK293FT cells. Lentivirus targeting green fluorescent protein (sense, AACGTACGCGGAATACTTCGA) was used as a control.

Antibodies

The following antibodies were used in this study: anti–acetyl-p53 (catalog no. 06-758, Millipore), anti-p53 (2524, Cell Signaling), anti-actin (ABT1485, Sigma), anti-NAMPT (MAB4044, R&D Systems), anti–phospho-p53 (9284, Cell Signaling), anti–phospho-S6 ribosomal protein (Ser 240/244) (5364S, Cell Signaling), anti–phospho-S6 ribosomal protein (Ser 235/236) (4858S, Cell Signaling), anti-S6 ribosomal protein (2317S, Cell Signaling), anti-histone H3 (ab10799, Abcam), anti-CD63 (sc-15363, Santa Cruz), anti-TSG101 (sc-7964, Santa Cruz), anti-γH2AX (NB100–384, Novus), anti-GPR94 (2104T, Cell Signaling), and anti-CD81 (ab109201, Abcam).

Mass Spectrometry

Methods linked to mass spectrometry identification of secreted proteins are found in the Supplementary Materials.

AdEV Purification and Size Analysis

AdEVs were isolated using the Total AdEV Isolation kit (catalog no. 4478359, Invitrogen) according to manufacturer's instructions. For size analysis, AdEVs were analyzed for size abundance distribution via optical imaging (Nanosight LM-10). We recorded five videos of 45 s for each sample, and data analysis was performed with NTA 1.1 software. Data are presented as the average and SD of five video recordings.

Electron Microscopy of AdEV

We applied 3 μL AdEV to formvar and carbon-coated copper grids (catalog no. FCF200-CU, EMS) and allowed to air dry. Grids were washed three times with water, incubated at room temperature for 3 min, and then 3 μL 1% phosphotungstic acid, pH 7.0 (EMS, catalog no. 19500) dissolved in water was applied to the grid. After 3 min, most of the phosphotungstic acid was removed by blotting with filter paper, and the remaining was allowed to air dry. Images were acquired using a JEOL1400+ transmission electron microscope operating at 80 kV, and a Gatan Orius 820 camera.

p53 Activity Determination

p53 DNA binding activity was measured using the p53 Transcription Factor Assay Kit (catalog no. 600020, Cayman) according to the manufacturer's directions.

RNA Purification and RT-PCR

Adipocytes were washed twice in cold PBS and total RNA was isolated by TRIzol reagent (catalog no. 15596018, Invitrogen) and 1 μg total RNA was reverse transcribed into cDNA using iScript (catalog no. 1708840, Bio-Rad), following the manufacturer's instruction. Transcription factor II E was used as an internal control to normalize expression. The following primers were used: transcription factor II E forward 5′- CAAG GCTTTAGGGGACCAGATAC-3′, transcription factor II E reverse 5′-CATCCATTGACTCCACAGTGACAC-3′; P16 forward 5′- GAACTCTTTCGGTCGTACCC-3′, p16 reverse 5′- CGAATC-TGCACCGTAGTTGA-3′; P21 forward 5′- GGTTCCTTGCCACTT-CTT-3′, p21 reverse 5′- GAGTCGGGATATTACGGTTG-3′; BAX forward 5′- AGGATGCGTCCACCAAGAAGCT-3′, BAX reverse 5′- TCCGTGTCCACGTCAGCAATCA-3′; BCL2 forward 5′- CCT-GTGGATGACTGAGTACCTG'-3′, BCL2 reverse 5′- AGCCAGGA-GAAATCAAACAGAGG-3′; Angptl4 forward 5′- GGAGATCCC-CAAGGCGAGTT-3′, Angptl4 reverse 5′- CAATTGGCTTCCTCGG-TTCC-3′; CXCL2 forward 5′- CTCCTTTCCAGGTCAGTTAGC-3′, CXCL2 reverse 5′- CAGAAGTCATAGCCACTCTCAA-3′; IGFBP7 forward 5′- GAGAAGGCCATCACCCAGGTCAGC-3′, IGFBP7 reverse 5′- GGATCCCGATGACCTCACAGCTCAAG-3′; and PAI-1 forward 5′- AGGATCGAGGTAAACGAGAGC-3′, PAI-1 reverse 5′- GCGGGCTGAGATGACAAA-3′.

Statistical Analysis

Statistical significance was determined using an unpaired, two-tailed Student's *t* test. All data in this article are expressed as mean ± SEM. Data presented have a sample size of three unless otherwise mentioned. Individual experiments were repeated at least three times.

Data and Resource Availability

All primary data and resources are available upon request.

RESULTS

Lipolysis Stimulates FABP4 and Vesicle Secretion

Previous studies showed that FABP4 secretion from adipocytes requires nutrient deprivation, lipolytic agonists, ATGL, and sirtuin 1 (15,16). To characterize the extent of lipolytic-dependent protein secretion, cultured adipocytes treated with the lipolytic stimulators, FSK, Iso, or Br-cAMP were evaluated for fatty acid release. Each of these treatments resulted in increased fatty acid secretion, whereas the ATGL inhibitor ASTAT significantly decreased basal lipid efflux (Fig. 1*A*). As previously shown, FSK treatment increased FABP4 and NAMPT secretion but did not lead to elevated DNA damage, as shown by unaltered γH2AX (Fig. 1*B*). Surprisingly, lipolytic activation resulted in secretion of vesicles, including the exosomal markers, CD63, TSG101, and CD81 (Fig. 1*B*). As a control, GRP94, an endoplasmic reticulum protein, was not present in the secreted exosomes. To further characterize the secretion of exosomes, nanoparticle tracking was used to determine the size and quantity of these vesicles. FSK stimulation resulted in approximately a twofold increase in vesicle release (Fig. 1*C*), and size analyses indicated a modest increase in the vesicles approximately 100 nm in diameter and a larger increase in vesicles approximately 130 nm in diameter (Fig. 1*D*). Furthermore, we evaluated the secreted vesicles by transmission electron microscopy, using a negative stain. Results showed vesicles with sizes consistent with the nanoparticle tracking analyses (Fig. 1*E*).

Concurrent with fatty acid and vesicle release, we also evaluated the protein content released from adipocytes after lipolytic stimulation. Coomassie-stained SDS-PAGE gels revealed a dramatic increase in the number of proteins secreted from adipocytes upon lipolytic stimulation of cultured 3T3-L1 adipocytes, as well as from primary murine adipocytes, with the total protein staining pattern appearing similar in both cultured and primary adipocyte cell models (Fig. 1*F*). The majority of secreted proteins from FSK-treated white adipose tissue (WAT) explants were found to remain in the supernatant after ultracentrifugation at 100,000*g* because few were detectable in the pellet fraction as assessed by a Coomassie-stained gel (Fig. 1*G*). Comparison by the protein compositional analysis (Fig. 1*G*) of the relative number of AdEV particles secreted after FSK stimulation (Fig. 1*D*) suggests that a major function of lipolytic stimulation of adipocytes is to load free and AdEV proteins into the secretory system.

To more fully characterize the proteins secreted by adipocytes in response to FSK stimulation, total secreted proteins from 3T3-L1 adipocytes were subjected to compositional analyses using mass spectrometry (Supplementary Table 1). A total of 289 unique proteins were identified (false discovery rate, <1%), of which 93% did not contain a classic secretion signal (Fig. 1*H*), consistent with an unconventional secretory mechanism. Analyses of the secreted proteins indicated that these proteins reside in the many subcellular locations and are involved in glucose and fatty acid metabolic pathways as well as protein translation, cytoskeleton, chaperone functions, and redox processes (Fig. 1*H*).

Lipolysis Activates AdEV and FABP4 Secretion Through a p53-Dependent Pathway

Najt et al. (22) showed that monounsaturated fatty acids produced by ATGL-dependent hydrolysis allosterically activate SIRT1, leading to deacetylation of protein targets. Moreover, Wang et al. (23) revealed that in adipocytes, p53 can be upregulated by nutrient starvation independently of senescence, apoptosis, or cell-death pathways. To assess if p53 plays a role in the nutritional stress–activated protein secretion system, we measured p53 activity in lipolytically activated 3T3-L1 adipocytes. As shown in Fig. 2*A*, p53 DNA–binding activity was significantly increased in response to Iso and Br-cAMP treatment, whereas ASTAT had no effect on basal p53 activity. Consistent with increased p53 transcriptional activity, the mRNA levels of the canonical p53 transcriptional targets BAX, BCL2, p16, and p21 were significantly increased in response to Iso treatment, an effect that was negated in the presence of ASTAT (Fig. 2*B*).

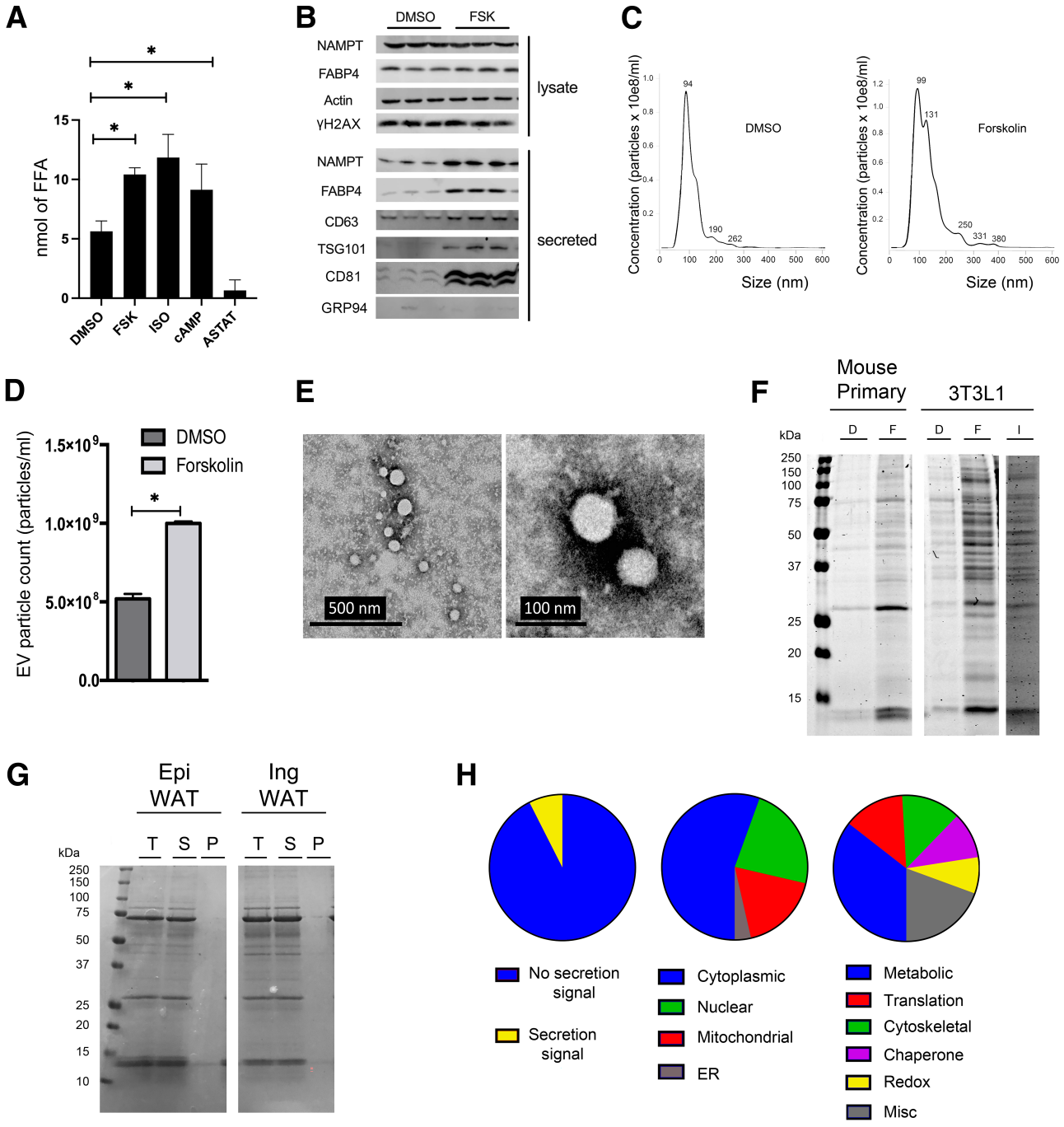

Figure 1—FSK stimulates protein secretion. *A*: Differentiated 3T3-L1 adipocytes were treated with DMSO, 10 μmol/L FSK, 10 μmol/L Iso, 1 mmol/L 8-Br-cAMP (cAMP in the figure) or 15 μmol/L ATGL inhibitor (ASTAT) for 4 h. Free fatty acid (FFA) levels in cell culture medium were measured and quantified by colorimetric assay. *B*: Differentiated 3T3-L1 adipocytes were treated with DMSO or 20 μmol/L FSK for 4 h. Whole-cell lysates were harvested, and equal amounts of intracellular protein underwent SDS-PAGE for Western blot analyses. For the secreted proteins, equal volumes of cell culture medium were loaded for Western blot analyses (NAMPT and FABP4). For the AdEV markers CD63, TSG101, and CD81, AdEVs were pelleted from equal volumes of cell culture medium, using the Total AdEV isolation reagent (catalog no. 4478359, Invitrogen). Subsequently, the pellets were lysed and resuspended into equal volume of RIPA buffer before analyses via Western blots. *C* and *D*: Differentiated 3T3-L1 adipocytes were treated with DMSO or FSK for 4 h and Nanosight analyses (see experiment details in *Research Design and Methods*) was used to quantify particle numbers (*C*) and AdEV particle size (*D*). *E*: 3T3-L1 adipocytes were treated with FSK for 4 h and AdEVs were pelleted using the Total AdEV isolation reagent. The AdEVs were negatively stained and mounted on a grid for transmission electron microscopy (46). *F*: Mouse primary and 3T3-L1 adipocytes were treated with FSK or Iso for 2 h and equivalent volumes were analyzed on SDS-PAGE and stained with Coomassie protein stain. *G*: C57Bl/6J mice were sacrificed and WAT was minced and washed. The explants were incubated in Krebs Ringer Bicarbonate Hepes (KRH) buffer with 10 μmol/L FSK for 2 h. The medium was recovered and ultracentrifuged at 100,000*g* for 1 h. The pellet was resuspended in the same volume of KRH. Equivalent volumes total protein (T), soluble (S), and pellet (P) were separated by SDS-PAGE and stained with Coomassie stain. Epi, epididymal; Ing, inguinal. *H*: Analyses of the mass spectrometry results of total FSK-dependent protein secretion, including percentage with classic secretion signals, subcellular locations, and functional pathways. Results represent the mean ± SEM. **P* < 0.05. EV, extracellular vesicle.

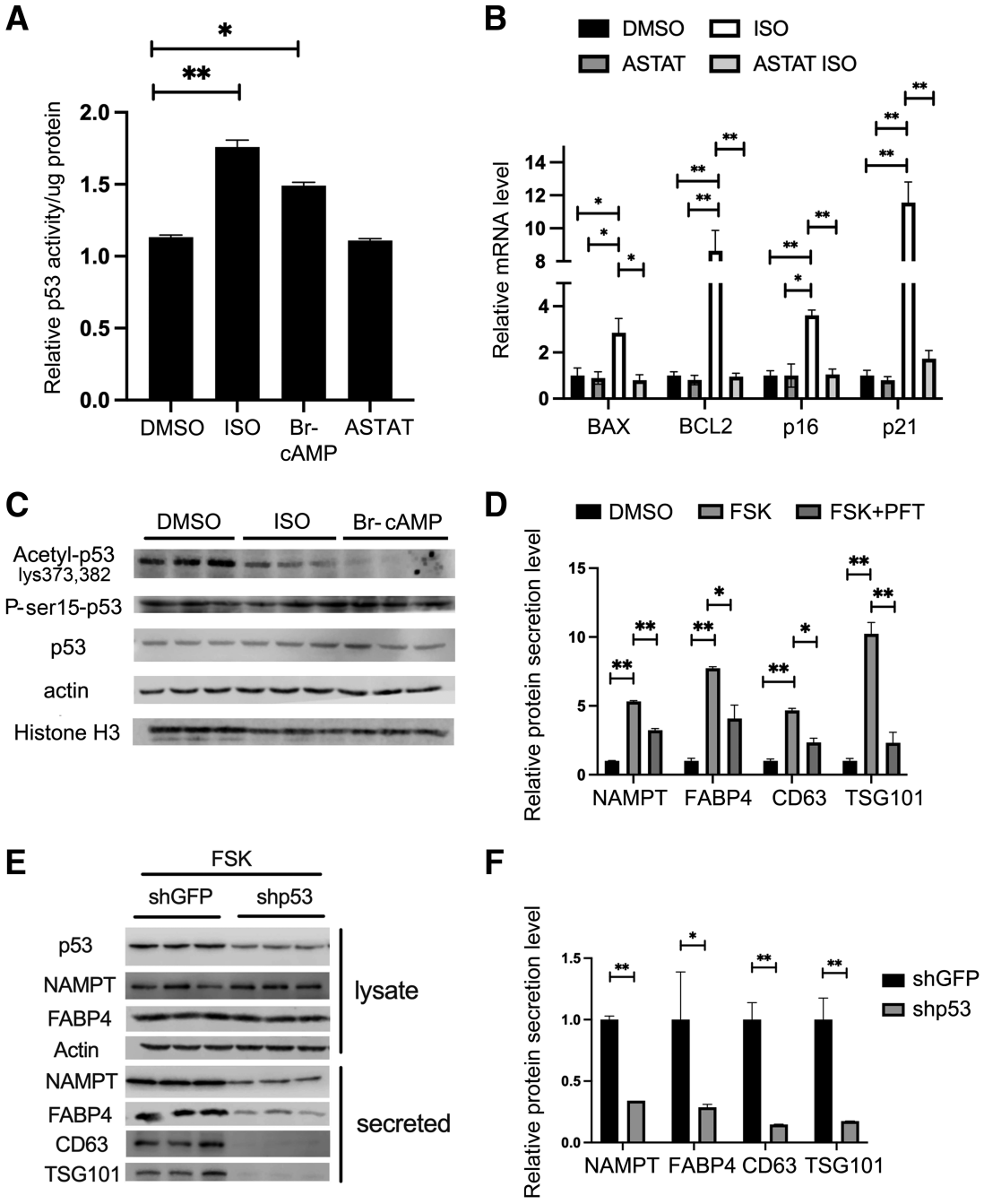

Figure 2—Lipolysis activates FABP4 and AdEV secretion through a p53-dependent pathway. *A*: Differentiated 3T3-L1 adipocytes were treated with DMSO, 10 μmol/L Iso, 1 mmol/L Br-cAMP, or 15 μmol/L ASTAT for 4 h. p53 Activity was measured using the p53 transcriptional factor assay kit (catalog no. 600020, Cayman) and the results were normalized to the concentration of whole-cell lysate protein. *B*: Differentiated 3T3-L1 adipocytes were pretreated with DMSO or 15 μmol/L ASTAT for 2 h, followed by DMSO or 10 μmol/L Iso for 4 h. RNA was purified and p53 transcriptional targets expression were measured by qRT-PCR. *C*: Differentiated 3T3-L1 adipocytes were treated with DMSO, 10 μmol/L Iso, or 1 mmol/L Br-cAMP for 4 h. Total protein was harvested and acetyl-p53, phospho-p53, total p53, actin, and histone H3 were measured by immunoblot analyses by loading equivalent protein. *D*: Differentiated 3T3-L1 adipocytes were pretreated with DMSO or 20 μmol/L PFT for 2 h, then were treated with DMSO or 20 μmol/L FSK for an additional 2 h. Western blot analyses were used to measure intracellular NAMPT, FABP4, and actin levels, as well as secreted protein levels (NAMPT, FABP4, CD63, and TSG101) in the cell culture medium. *E*: Genetic knockdown of p53 (shp53) and control (shGFP) were made in 3T3-L1 cell lines by lentiviral transduction. The cells were treated with 20 μmol/L FSK for 4 h. Western blot analyses were used to measure intracellular p53, NAMPT, FABP4, and actin levels, as well as secreted protein levels (NAMPT, FABP4, CD63, and TSG101) in the cell culture medium. In all these experiments, the intracellular lysate was prepared from harvesting whole cells, and equal amounts of intracellular protein were loaded onto SDS-PAGE gels for immunoblots. For secreted samples, equal volumes of cell culture medium were used. For the AdEV markers CD63 and TSG101, AdEVs were pelleted from an equal volume of the cell culture medium, using a total AdEV isolation reagent (catalog no. 4478359, Invitrogen). The pellets were lysed and resuspended into an equal volume of RIPA buffer. *F*: Quantification of the protein secretion in p53 knockdown shown in *D*. All results represent the mean ± SEM. $*P < 0.05$, $**P < 0.01$.

Recently, Huang et al. (24) have shown that in macrophages, fatty acids derived from either intracellular triglyceride hydrolysis or the de novo pathway could activate SIRT1 leading to the deacetylation of p53. To determine if p53 was similarly regulated in adipocytes, we evaluated p53 acetylation after lipolytic activation. Figure 2*C* reveals that concomitant with lipolytic stimulation, p53 is deacetylated. Deacetylation of p53 is typically considered inhibitory toward transcriptional control, yet our results suggested activation of p53 DNA–binding activity (Fig. 2*A*). This suggested that additional, possibly covalent, modifications of p53 may be occurring coincident with nutritional stress. To that end, we assessed the phosphorylation status of p53 at Ser15 after Iso or Br-cAMP administration. Fig. 2*C* shows that while acetylation decreases with lipolytic stimulation, phosphorylation of p53 at Ser15 was largely unaffected, suggesting that other, unidentified processes increase p53 activity after lipolytic stimulation.

To further assess if p53 plays a role in lipolytic-dependent protein secretion in adipocytes, differentiated 3T3-L1 adipocytes were pretreated with the p53 inhibitor pifithrin-α (PFT) for 2 h followed by FSK stimulation. Consistent with previous results (16), FSK treatment alone significantly increased protein secretion from adipocytes, as shown by release of FABP4 (non-AdEV), CD63, TSG101, and NAMPT (AdEV resident proteins). However, inhibition of p53 activity by PFT significantly reduced FSK-stimulated FABP4 and AdEV secretion (CD63, TSG101, and NAMPT) (Fig. 2*D*). As a complimentary strategy to chemical inhibition, we tested a genetic model using stably silenced p53. Silencing of p53 in 3T3-L1 adipocytes resulted in cells with markedly diminished secretion of exosomal or nonexosomal protein after FSK treatment (Fig. 2*E* and 2*F*). Together, these data suggest that loss of p53 activity or reduction in p53 abundance significantly diminishes FABP4 and AdEV secretion (CD63, TSG101, and NAMPT) from adipocytes.

Previous studies have shown that FABP4 is secreted largely by adipocytes (16) and that the circulating level of FABP4 represents a function linked to fat cells and not macrophages. Because of this, we evaluated the level of serum FABP4 from p53-null mice as an indicator of adipocyte secretion. Figure 3*A* shows that the circulating level of FABP4 was significantly reduced in whole-body, p53-null male mice serum compared with that of wild-type littermates. Consistent with a role for p53 in AdEV secretion, the number of exosomal particles was significantly reduced in p53-null male mice serum compared with that of wild-type controls, although the size of the AdEVs was not significantly altered (Fig. 3*B*). Overall, our data suggest that activation of p53 facilitates FABP4 and AdEV protein secretion in both cultured adipocytes and in adipose tissue from experimental mice.

To further assess the role of p53 in adipocyte protein secretion, we used a gain-of-function strategy evaluating whether a small-molecule p53 activator would lead to protein secretion independent of the upstream lipolytic dependence. Nutlin is an MDM2 inhibitor functioning as a p53 activator (25). When differentiated 3T3-L1 adipocytes were treated with nutlin, the secretion of FABP4 and AdEVs (CD63, TSG101, and NAMPT) were significantly increased (Fig. 4*A*). To further determine whether nutlin activation of p53 increased the secretion of the complex pool of proteins seen in lipolytically induced adipocyte protein secretion, we evaluated the nutlin-induced secreted material using Coomassie-stained SDS-PAGE. The results show that proteins of many sizes are increased upon nutlin treatment (Fig. 4*B*). As an indication of the effectiveness of

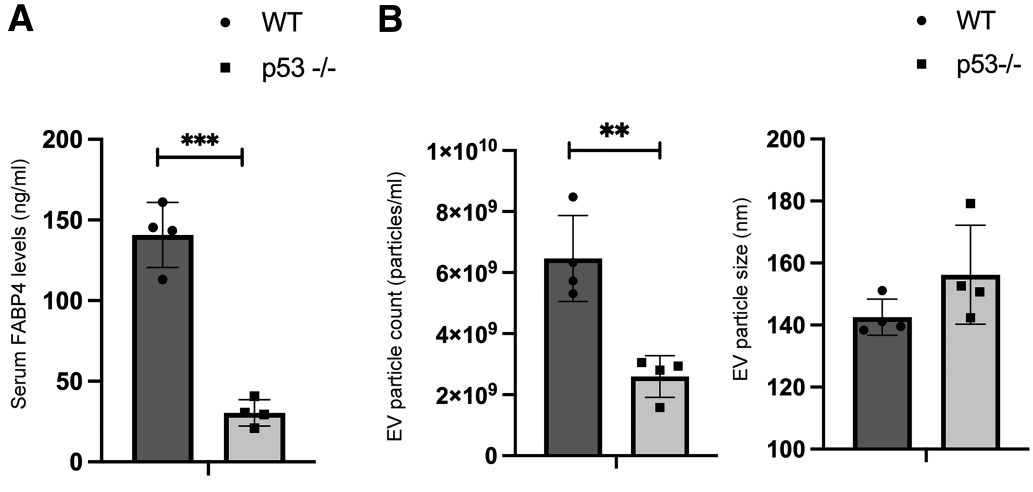

Figure 3—FABP4 and AdEV protein secretion from adipocytes is decreased in p53-null mice. *A*: ELISA was used to measure FABP4 levels in 8-week-old, male, wild-type (WT) or p53-null mice serum. Serum from p53-null mice (obtained at 6 P.M. during the light phase) was evaluated for FABP4 levels. *B*: AdEVs were pelleted, purified from an equal volume of mouse serum from 8-week-old, male, WT or p53-null mice and resuspended in 1 mL PBS for analyses. AdEV size and amounts were measured by Nanosight analysis (see experiment details in *Research Design and Methods*). All results represent the mean ± SEM. $^{**}P < 0.01$, $^{***}P < 0.001$. EV, extracellular vesicle.

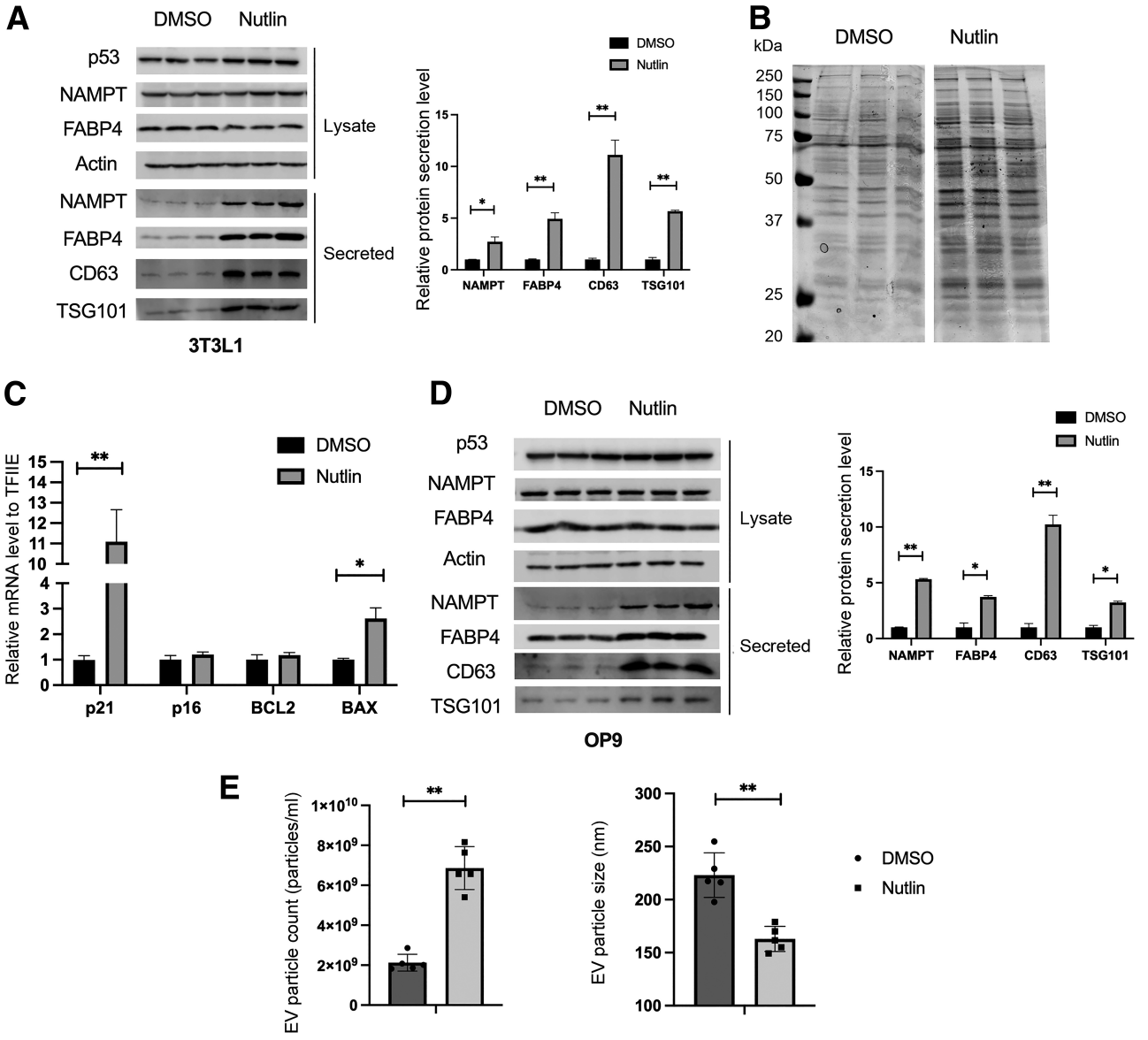

Figure 4—p53 facilitates FABP4 and AdEV protein secretion from adipocytes. *A*: Differentiated 3T3-L1 adipocytes were treated with DMSO or 10 μmol/L nutlin for 48 h. Western blot analysis was used to measure intracellular levels of the proteins p53, NAMPT, FABP4, and actin levels, as well as secreted protein level (NAMPT, FABP4, CD63, and TSG101) in the cell culture medium. *B*: Differentiated 3T3-L1 adipocytes were treated with DMSO or 10 μmol/L nutlin for 24 h. Equivalent volumes of culture medium were analyzed on SDS-PAGE gels and proteins were stained with Coomassie protein stain. *C*: Differentiated 3T3-L1 adipocytes were treated with DMSO or 10 μmol/L nutlin for 48 h. RNA was purified and expression of p53 transcriptional targets was measured by qRT-PCR. *D*: Differentiated OP9 adipocytes were treated with DMSO or 10 μmol/L nutlin for 24 h. Western blot analysis was used to measure intracellular protein p53, NAMPT, FABP4, and actin levels, as well as secreted protein level (NAMPT, FABP4, CD63, and TSG101) in the cell culture medium, as in *A*. *E*: Differentiated 3T3-L1 adipocytes were treated with DMSO or 10 μmol/L nutlin for 48 h. AdEVs were pelleted, purified from equal volume of cell culture medium from different treatment, and resuspended in 1 mL PBS for future analysis. AdEV size and amounts were measured by Nanosight analysis (see experiment details in *Research Design and Methods*). All results represent the mean ± SEM. **P* < 0.05, ***P* < 0.01. EV, extracellular vesicle.

nutlin treatment, the mRNA levels of canonical p53 transcriptional targets BAX and p21 were also significantly increased (Fig. 4*C*). To ensure that the regulation of secretion by p53 was not system specific, we repeated the nutlin treatment in OP9 (26) adipocytes and similarly found that FABP4 and AdEV secretion (CD63, TSG101, and NAMPT) were markedly increased (Fig. 4*D*). Interestingly, in response to nutlin treatment, although the number of exosomal particles was elevated threefold, the diameter of the AdEVs was markedly reduced (Fig. 4*E*).

DNA Damage Facilitates FABP4 and AdEV Protein Secretion From Adipocytes

As a master transcriptional regulator of the cellular stress response, p53 is canonically activated through DNA damage (27,28), increasing either p53 protein expression and/or

p53 DNA–binding activity. To assess if DNA damage in adipocytes, a terminally differentiated nongrowing cell, would activate p53, 3T3-L1 adipocytes were treated with the DNA-damage inducer DOXO and secretion was evaluated. As shown in Fig. 5*A*, DOXO treatment stimulated FABP4 and AdEV secretion coincident with induction of γH2AX. As a positive control for DNA damage, p53 protein levels were increased with DOXO treatment (Fig. 5*A*). Similar to the results with nutlin activation of p53, DOXO treatment resulted in secretion of more AdEVs, but their average diameter was markedly reduced (Fig. 5*B*).

To further assess whether DOXO-induced protein secretion in 3T3-L1 adipocytes upregulated p53 activity, the mRNA levels of the canonical p53 transcriptional targets BAX, BCL2, p16, and p21 were measured. Figure 5*C* shows that some (p16 and BAX; a trend for p21) were increased in response to DOXO treatment. Additionally, when OP9 adipocytes were treated with DOXO, AdEV particle secretion was also increased. In contrast, pretreatment with the p53 inhibitor PFT resulted in attenuated DOXO-stimulated AdEV secretion, implicating the p53-dependence of DNA-damage-induced protein secretion (Fig. 5*D*). It is well known that DOXO is an inducer of senescence (29). However, the adipocyte protein secretion pathway is an acute process, occurring with hours of treatment, whereas senescence is a slower process, typically occurring over the course of 1–3 weeks. To evaluate if protein secretion induced by DOXO treatment was linked to senescence-associated protein secretion, markers of senescence were monitored. For this, β-galactosidase activity and additional markers of senescence were measured (30,31). Importantly, β-galactosidase activity was not increased with DOXO treatment, expression of one senescence-associated gene was unchanged (CXCL2), one was increased (IGFBP7), and two others (Angptl4 and Pai1) were downregulated (Supplementary Fig. 1). As such, although DOXO is a senescence inducer in some systems, under the acute experimental conditions used here, activation of cellular senescence is unlinked to AdEV secretion.

To compare genotoxic DNA damage with genetic potentiation, ERCC1 haploinsufficient mice were used. ERCC1-XPF is an endonuclease that plays a vital role in all three major DNA repair processes (i.e., nucleotide excision repair, interstrand cross-link repair, double strand break repair) (32,33). Although ERCC1-XPF–null mice are embryonic lethal, $ERCC1^{-/\Delta}$–haploinsufficient animals exhibit markedly reduced DNA repair and increased genomic DNA damage, thus serving as a model for age-related pathophysiologies (32,33). Potentiated DNA damage upregulates p53 (34) and, as shown in Fig. 6*A*, the level of circulating FABP4 was significantly increased in the serum from whole-body $ERCC1^{-/\Delta}$ male mice as compared with the wild type. Surprisingly, there was no significant difference in the level of circulating FABP4 level in the serum of female $ERCC1^{-/\Delta}$ mice (Fig. 6*A*), which suggests that sex differences might also play an important role in the adipocyte unconventional secretion process. The sex difference in circulating FABP4 was likely not due to the level of lipolysis in adipose tissue, because the levels of circulating free fatty acids were not different between male and female $ERCC1^{-/\Delta}$ samples (Fig. 6*B*). Consistent with DNA damage resulting in activated p53, the protein expression of p53 was increased in both depots of $ERCC1^{-/\Delta}$ male mice, but surprisingly, the γH2AX level was only increased in the visceral fat tissue (Fig. 6*C*). Furthermore, the mRNA level of the canonical p53 transcriptional targets BCL2 and BAX were significantly increased in the visceral but not the subcutaneous adipose tissue depot of $ERCC1^{-/\Delta}$ male mice, as compared with the wild-type controls (Fig. 6*D*). Overall, these data suggest that DNA damage facilitates protein secretion in a p53-dependent manner in adipocytes.

The p53 Downstream Target mTOR Links Nutrient Sensing to Adipocyte Protein Secretion

Previous studies have shown that FABP4 secretion from adipocytes is dependent on some, but not all, components of autophagy and, in particular, the ULK1 kinase complex (16). The mammalian target of rapamycin (mTOR) is one of the major sensors of nutrient starvation and is a crucial negative regulator of autophagy (35,36). Treatment of 3T3-L1 adipocytes with the p53 activator nutlin (Fig. 7*A*) or the DNA-damage agent DOXO (Fig. 7*B*) reduced mTOR activity as assessed by phosphorylation of S6 (Ser 235/236 and 240/244) and concomitantly increased protein secretion (Fig. 4*A*, 5*A*). Similarly, when 3T3-L1 adipocytes were treated with pharmacological inhibitors of mTOR (torin or rapamycin), FABP4 and AdEV secretion (CD63, TSG101, and NAMPT) was significantly increased (Fig. 7*C*). In this case, the number of secreted exosomal particles was increased, whereas the size of AdEVs was unaffected by mTOR inhibition (Fig. 7*D*). Overall, these data suggest that mTOR serves as a regulatory target of p53 linking its nutrient-sensing function to control of autophagy and secretion.

DISCUSSION

Adipose tissue secretes numerous paracrine and endocrine factors, including cytokines, hormones, extracellular vesicles, signaling lipids, and adipokines in response to hormonal or nutritional cues (3). Obesity has been identified as a major risk factor for the development of several cancers, including breast, colorectal, and pancreatic (21). Elevated circulating levels of FABP4 have been demonstrated in women with breast cancer as compared with healthy control individuals (37,38), and elevated expression of FABP4 is also significantly correlated with recurrence and disease-free survival; in mouse models, tumor progression is significantly decreased in whole-body FABP4 knockouts (37,39).

Adipocyte release of AdEVs has been noted by several groups (8,40), revealing that adipocytes can release a variety of sizes of vesicles, with some up to 1,500 nm, and including whole mitochondria (8,11,12). Our nanoparticle analyses only profiled smaller vesicles (<600 nm). The studies reported herein demonstrate that release of these AdEVs is regulated by lipolysis in a time frame equivalent

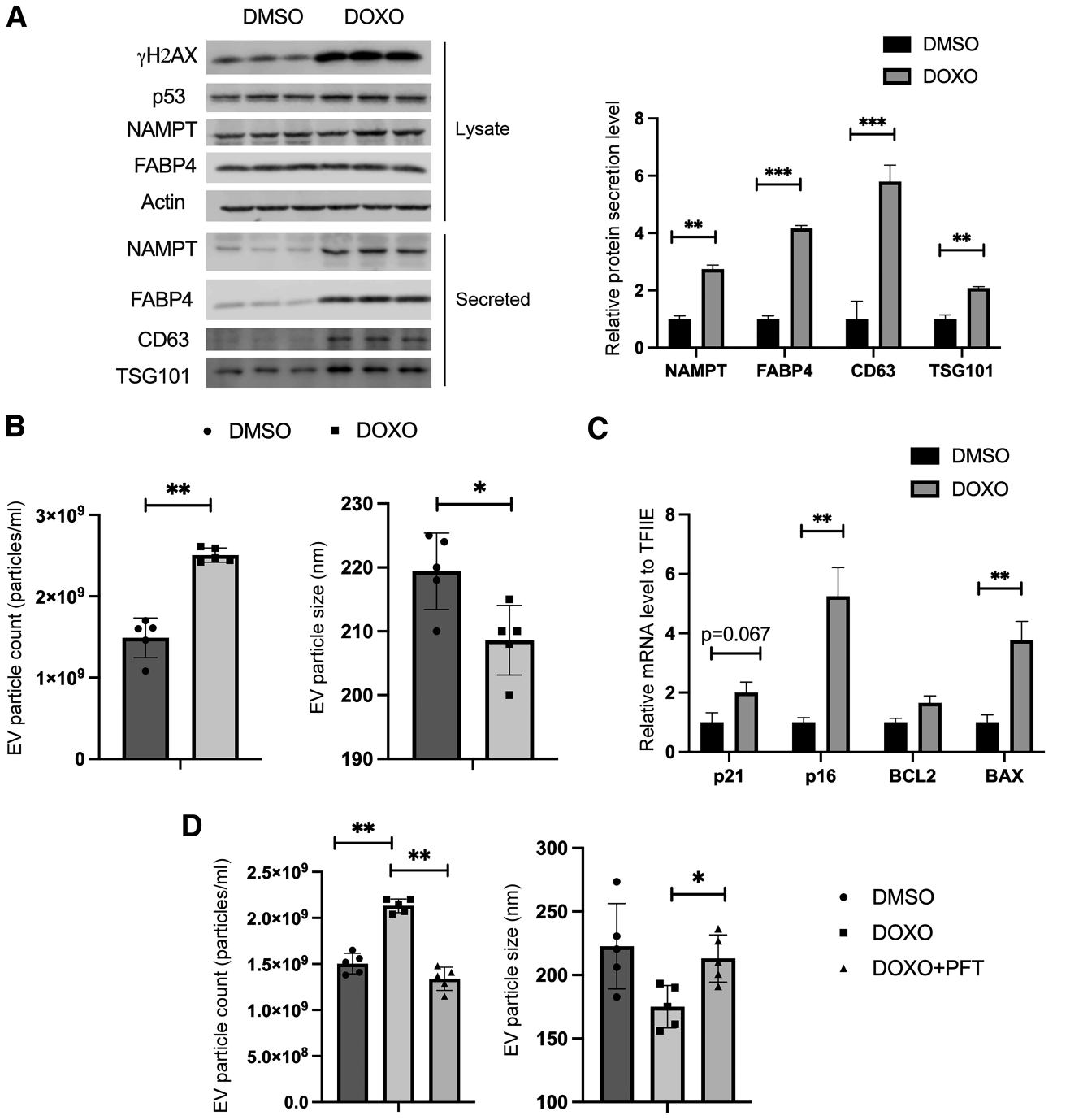

Figure 5—DNA damage facilitates FABP4 and AdEV protein secretion from adipocytes in a p53-dependent manner. *A*: Differentiated 3T3-L1 adipocytes were treated with DMSO or 10 μmol/L DOXO for 24 h. Western blot analysis was used to measure intracellular levels of the proteins γH2AX, p53, NAMPT, FABP4, and actin, as well as secreted protein level (NAMPT, FABP4, CD63, and TSG101) in the cell culture medium. For the intracellular lysate, whole-cell lysates were harvested for each condition and equal amounts of intracellular protein were loaded to Western blots. For the secreted samples, equal volumes of cell culture medium were loaded onto Western blots. For the AdEV markers CD63 and TSG101, AdEVs were pelleted from an equal volume of cell culture medium, using the Total AdEV isolation reagent. The pellets were lysed and resuspended into an equal volume of RIPA buffer before loading to Western blots. *B*: Differentiated 3T3-L1 adipocytes were treated with DMSO or 10 μmol/L DOXO for 24 h. AdEVs were pelleted from an equal volume of cell culture medium and resuspended in 1 mL PBS for future analyses. AdEV size and amounts were measured by Nanosight analyses (see experiment details in *Research Design and Methods*). *C*: Differentiated 3T3-L1 adipocytes were treated with DMSO or 10 μmol/L DOXO for 24 h. The RNA was purified and p53 transcriptional targets expression was measured by qRT-PCR. *D*: Differentiated OP9 adipocytes were pretreated with DMSO or 20 μmol/L PFT for 2 h, then treated with DMSO or 10 μmol/L DOXO for 24 h. AdEVs were pelleted, purified from equal volume of cell culture medium from different treatment, and resuspended in 1 mL PBS for analysis. AdEV size and amounts were measured by Nanosight analysis (see experiment details in *Research Design and Methods*). All results represent the mean ± SEM. $^*P < 0.05$, $^{**}P < 0.01$, $^{***}P < 0.001$. EV, extracellular vesicle.

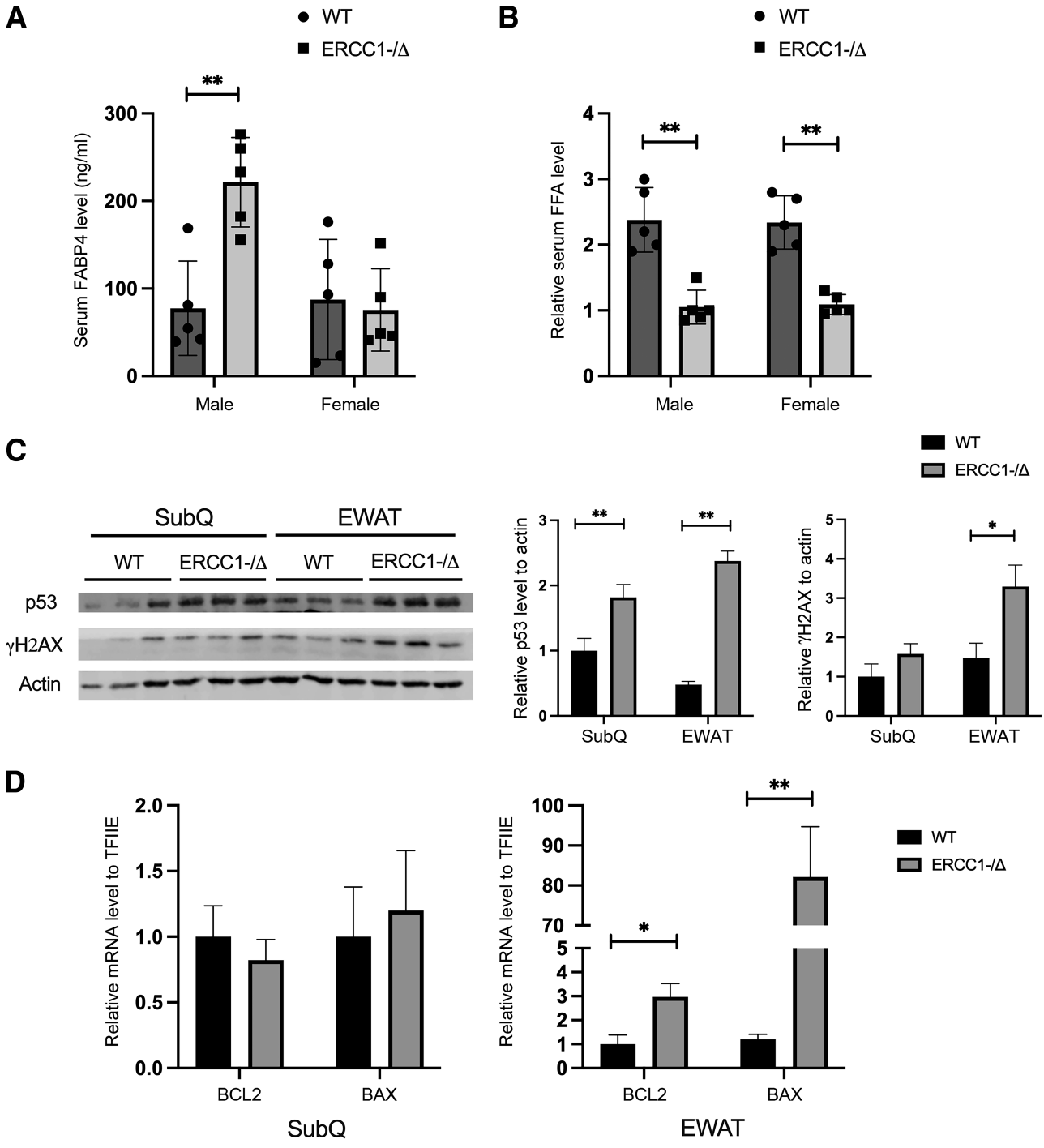

Figure 6—DNA damage facilitates FABP4 and AdEV protein secretion from adipocytes in ERCC1$^{-/\Delta}$ mice. *A*: FABP4 levels were quantified in 20-week-old male and female wild-type (WT) or ERCC1$^{-/\Delta}$ mice serum using an ELISA assay. Equal amounts of serum were used for the ELISA. *B*: Levels of serum free fatty acids (FFAs) in 20-week-old male and female WT or ERCC1$^{-/\Delta}$ mice were measured and quantified by colorimetric assay. Equal volumes of serum were used for the measurements. *C*: Visceral (EWAT) and subcutaneous adipose tissue (SubQ) were harvest from 16-week-old male WT and ERCC1$^{-/\Delta}$ mice. Whole-cell lysates were harvested, and Western blots were performed to measure p53, actin, and γH2AX in 16-week-old male WT and ERCC1$^{-/\Delta}$ mice. *D*: EWAT and SubQ were harvested from 16-week-old male WT and ERCC1$^{-/\Delta}$ mice. The RNA was purified and expression of p53 transcriptional targets was measured by qRT-PCR. All results represent the mean ± SEM. $^{*}P < 0.05$, $^{**}P < 0.01$.

to that for lipolysis-regulated fatty acid release. Unexpectedly, 3T3-L1 adipocytes release AdEV particles basally (no lipolytic stimulation), although these are largely devoid of significant protein content. Upon stimulation, the release of AdEV particles only increased twofold, whereas released protein content was dramatically increased. It is unclear what other molecules are contained in these AdEVs, such as miRNA, organelles, DNA, or lipids. Similar to the work by

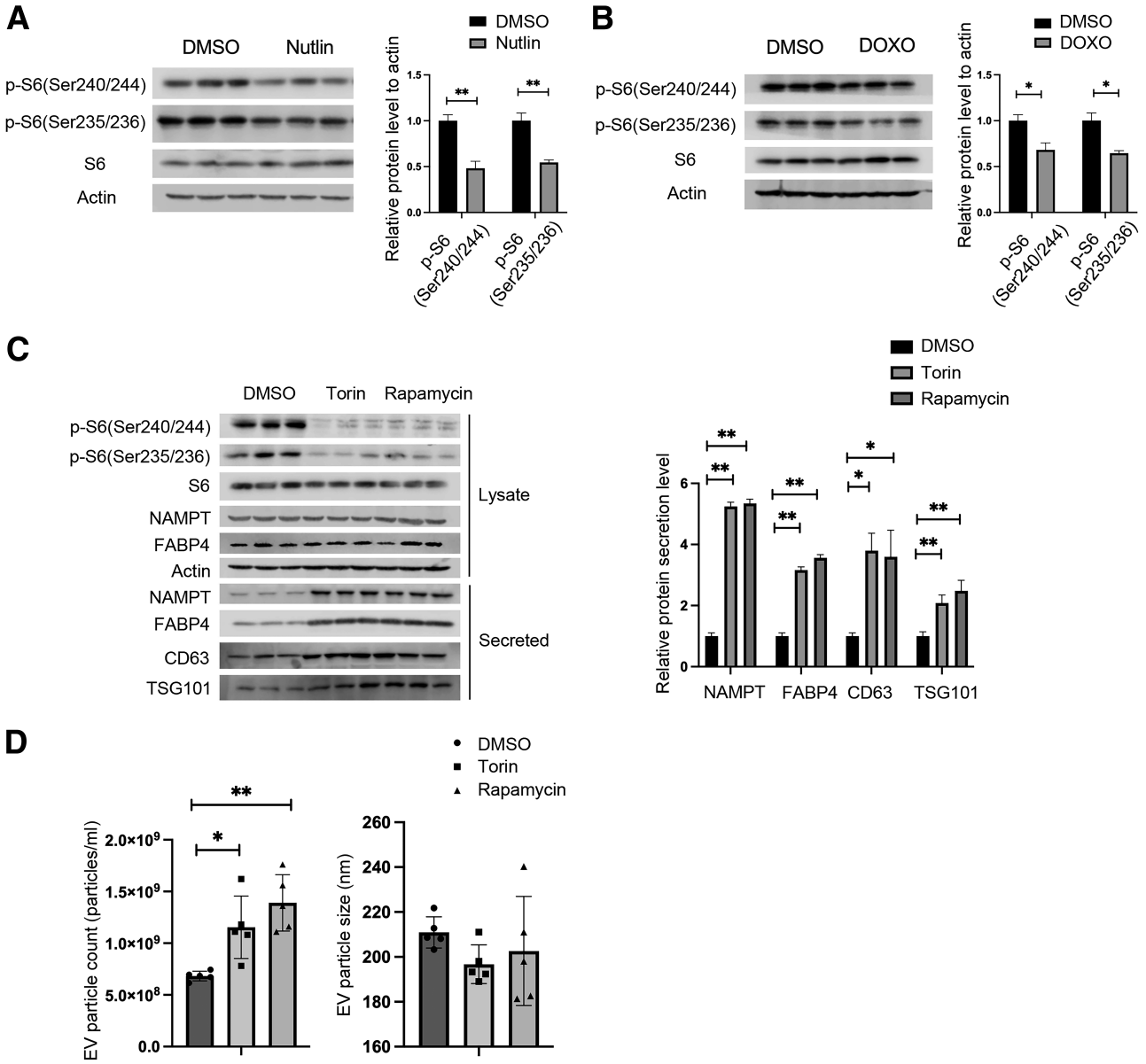

Figure 7— mTOR is inhibited by p53 and further inhibits FABP4 and AdEV protein secretion from adipocytes. *A*: Differentiated 3T3-L1 adipocytes were treated with DMSO or 10 μmol/L nutlin for 48 h. Western blot analyses were used to measure intracellular phospho-S6 (Ser 240/244), phospho-S6 (Ser 235/236), S6, and actin levels. *B*: Differentiated 3T3-L1 adipocytes were treated with DMSO or 10 μmol/L DOXO for 24 h. Western blot analyses were used to measure intracellular Ser 240/244, Ser 235/236, S6, and actin levels. *C*: Differentiated 3T3-L1 adipocytes were treated with torin and rapamycin for 24 h. Western blot analyses were used to measure intracellular protein Ser 240/244, Ser 235/236, S6, NAMPT, FABP4, and actin levels, as well as secreted protein levels (NAMPT, FABP4, CD63, and TSG101) in the cell culture medium. For the intracellular lysate, whole-cell lysates were harvested for each condition and equal amounts of intracellular protein were loaded to Western blots. For the secretion analyses, equal volumes of cell culture medium were loaded onto Western blots. For the AdEV markers CD63 and TSG101, AdEVs were pelleted from equal volumes of cell culture medium by using Total AdEV isolation reagent. The pellets were lysed and resuspended in equal volumes of RIPA buffer before loading onto Western blots. *D*: Differentiated 3T3-L1 adipocytes were treated with torin and rapamycin for 24 h. AdEVs were pelleted, purified from an equal volume of cell culture medium from different treatments, and resuspended in 1 mL PBS for future analyses. AdEV size and amounts were measured by Nanosight analyses. All results represent the mean ± SEM. $*P < 0.05$, $**P < 0.01$. EV, extracellular vesicle.

Flaherty et al. (9), who characterized triglyceride-containing AdEVs from adipose tissue and their uptake by resident macrophages, vesicles isolated from lipolytically stimulated 3T3-L1 or murine adipose tissue cannot be collected via ultracentrifugation. In contrast to our work, secretion of AdEVs from *Lep*$^{ob/ob}$ mice did not require ATGL, and the particles are generally smaller in diameter than those secreted from 3T3-L1 or OP9 adipocytes (9). Further work will be necessary to assess the different metabolic and procedural conditions affecting AdEV secretion and properties.

Previous work by Durcin et al. (8) identified that, basally, 3T3-L1 adipocytes secrete two size classes of extracellular

vesicles that have similar protein composition but vary markedly in their phospholipid and cholesterol content. Even though the data reported by Durcin et al. (8) relied on centrifugation preparations and longer collection times, we identified many of the same proteins in our lipolytic dependent secretion samples (Supplementary Table 1). Recent published data have shown that adipocytes and other cell types release whole mitochondria (11,12). Some of these are composed of oxidized mitochondria that, after release, become degraded by macrophages (11). In brown adipocytes, uptake and metabolism of AdEVs is necessary to allow efficient thermogenesis (41). An alternative rationale for mitochondria release has been proposed that suggests secreted mitochondria support the survival of metabolically compromised cells (11) and that adipocytes secrete functional mitochondria as a mechanism for cellular homeostasis. Figure 1*G* shows that the adipocyte lipolytic secretome contains many proteins annotated as mitochondrial. It is not clear if this represents active or inactive mitochondrial content or secretion of mitochondrial proteins devoid of membranes.

Importantly, the work reported herein focuses on the role of p53 in hormone-stimulated protein or AdEV secretion. Our studies provide a more detailed molecular mechanism of how DNA damage or nutrient deprivation (lipolysis) promotes AdEV and protein secretion, including increased p53 DNA–binding activity that leads to increased adipocyte AdEV and protein secretion. Consistent with this, Wang et al. (23) reported that p53 expression and activity can be markedly upregulated by nutrient starvation but was unlinked to cell senescence, apoptosis, or any death-related p53 canonical pathway. Najt et al. (22) have shown that lipolytically released fatty acids, specifically monounsaturated fatty acids, allosterically activate SIRT1, leading to downstream protein deacetylation. Consistent with this model, Huang et al. (24) showed that in macrophages, monounsaturated fatty acids decreased p53 acetylation, DNA binding, and transcriptional activity. Paradoxically, the activation of lipolysis in adipocytes is associated with increased expression of p53 target genes (namely, BAX, BCL2, p16, and p21) implying other mechanisms linked to triglyceride hydrolysis may activate p53. Our studies suggest that nutrient stress is an activating signal for p53 in adipocytes and that this process may be independent of p53 phosphorylation at Ser15 (Fig. 2*C*). There may be other unappreciated phosphorylations and modifications of p53 that influence DNA binding activity as well.

Activation of p53 by lipolytic agents or pharmacologically with nutlin increased AdEV and protein secretion. Consistent with this, inhibition of p53 via silencing or genetic loss resulted in attenuated secretion (Fig. 2*E* and 2*F*). Interestingly, although FABP4 is largely secreted by fat cells, the total number of circulating extracellular vesicles was decreased in serum from whole-body p53-null mice, implying that either adipocytes are a major secretory system for circulating vesicles or p53 plays a fundamental role in vesicular secretion in other cells as well. Consistent with this, oncogenic p53 mutations upregulate the tumor secretome in a number of systems, leading to p53-dependent delivery of miRNAs and other signaling molecules within the tumor microenvironment.

p53 Activation after DNA damage similarly increased AdEV and protein secretion. This was revealed using either chemical (DOXO) or genetic ($ERCC1^{-/\Delta}$) potentiation. In cultured OP9 adipocytes, activation of AdEV secretion by DOXO was attenuated by the p53 inhibitor PFT. In 3T3-L1 adipocytes, DOXO activated p53-dependent gene expression and increased protein and AdEV particle secretion. Using the ERCC1 haploinsufficient mouse system, activation of p53 (42) resulted in increased circulating FABP4. Interestingly, $ERCC1^{-/\Delta}$ mice have markedly reduced body fat and have reduced lipolysis and circulating fatty acids, yet increased protein secretion, suggesting that even though lipolysis is diminished in this system, the activation of p53 by DNA damage potentiates secretion.

Interestingly, both lipolysis and DNA damage lead to activation of p53. We have shown that a lipolytic stimulus does not lead to increased DNA damage as monitored by γH2AX foci. Moreover, fasting does not cause DNA damage; it increases DNA repair (43). It should be noted that although acute lipolysis does not cause DNA damage, chronic DNA damage can increase lipolysis. As such, the acute regulatory events studied here suggest that the activation of p53 from lipolysis and DNA damage are independent.

Prior work by Josephrajan et al. (16) revealed that FABP4 secretion required components of the ULK1 autophagy complex, including ULK1, FIP200, and Beclin1/ATG6. The ULK1 complex is negatively regulated by mTORC1 such that during nutrient availability, mTORC1-dependent phosphorylation restricts autophagic flux. As shown in Fig. 7, inhibition of mTORC1 using rapamycin or torin similarly potentiated protein and AdEV secretion in both 3T3-L1 and OP9 adipocytes. This implies that not only does nutrient starvation increase AdEV secretion but nutrient abundance and insulin attenuate AdEV secretion, making adipocyte secretion a highly dynamic process.

TP53-derived cancers are correlated with adipocyte lipolysis. Kang et al. (44) generated a p53 R178C knock-in mouse modeling the human TP53 R181C mutation characterized by Li-Fraumeni syndrome. This mouse has a lean phenotype and increased adipocyte lipolysis. In general, p53 promotes fatty acid oxidation and plays a significant role in the expression of genes linked to mitochondrial lipid metabolism, including Lipin1, peroxisomal carnitine *O*-octanoyltransferase, carnitine palmitoyltransferase, acyl-CoA dehydrogenase, and malonyl-CoA decarboxylase (reviewed by Laubach et al. (45)). Several cancers (e.g., ovarian cancer, pancreatic cancer) use fatty acids as major fuels; therefore, it is likely that during oncogenic lipolysis, not only are fatty acids released by adipocytes but also protein and extracellular vesicles. TP53 gain-of-function mutations that diminish interaction with MDM2 and result in

increased p53 levels may potentiate AdEV secretion, whereas loss-of-function mutations in p53 would be anticipated to attenuate AdEV secretion. Future work will test this hypothesis.

Funding. This work was supported by the National Institutes of Health (grant DK053189 to D.A.B.). A portion of this work was carried out in the Minnesota Nano Center, which receives partial support from the National Science Foundation through the National Nanotechnology Coordinated Infrastructure program.

Duality of Interest. No potential conflicts of interest relevant to this article were reported.

Author Contributions. Y.H. developed the experimental plan, conducted experiments, and wrote the manuscript. A.V.H. developed the experimental design, carried out experiments, wrote the manuscript, and prepared the figures. S.R.F., C.L.H., and E.K.B. carried out experiments and edited the manuscript. H.M.M. carried out the experimental plan and edited the manuscript, C.C.D. conducted experiments and edited the manuscript, R.S.H. developed the experimental plan and edited the manuscript. M.A.S. conducted experiments and wrote the manuscript, L.J.N. developed the experimental plan and edited the manuscript. D.A.B. conceived the study, reviewed the results, and wrote the manuscript. D.A.B. is the guarantor of this work and, as such, had full access to all the data in the study and takes responsibility for the integrity of the data and the accuracy of the data analysis.

References

1. Choe SS, Huh JY, Hwang IJ, Kim JI, Kim JB. Adipose tissue remodeling: its role in energy metabolism and metabolic disorders. Front Endocrinol (Lausanne) 2016;7:30
2. Rosen ED, Spiegelman BM. Adipocytes as regulators of energy balance and glucose homeostasis. Nature 2006;444:847–853
3. Wozniak SE, Gee LL, Wachtel MS, Frezza EE. Adipose tissue: the new endocrine organ? A review article. Dig Dis Sci 2009;54:1847–1856
4. Roca-Rivada A, Alonso J, Al-Massadi O, et al. Secretome analysis of rat adipose tissues shows location-specific roles for each depot type. J Proteomics 2011;74:1068–1079
5. Kwan HY, Chen M, Xu K, Chen B. The impact of obesity on adipocyte-derived extracellular vesicles. Cell Mol Life Sci 2021;78:7275–7288
6. Valadi H, Ekström K, Bossios A, Sjöstrand M, Lee JJ, Lötvall JO. Exosome-mediated transfer of mRNAs and microRNAs is a novel mechanism of genetic exchange between cells. Nat Cell Biol 2007;9:654–659
7. Lazar I, Clement E, Dauvillier S, et al. Adipocyte exosomes promote melanoma aggressiveness through fatty acid oxidation: a novel mechanism linking obesity and cancer. Cancer Res 2016;76:4051–4057
8. Durcin M, Fleury A, Taillebois E, et al. Characterisation of adipocyte-derived extracellular vesicle subtypes identifies distinct protein and lipid signatures for large and small extracellular vesicles. J Extracell Vesicles 2017;6:1305677
9. Flaherty SE 3rd, Grijalva A, Xu X, Ables E, Nomani A, Ferrante AW Jr. A lipase-independent pathway of lipid release and immune modulation by adipocytes. Science 2019;363:989–993
10. Crewe C, Joffin N, Rutkowski JM, et al. An endothelial-to-adipocyte extracellular vesicle axis governed by metabolic state. Cell 2018;175:695–708.e13
11. Brestoff JR, Wilen CB, Moley JR, et al. Intercellular mitochondria transfer to macrophages regulates white adipose tissue homeostasis and is impaired in obesity. Cell Metab 2021;33:270–282.e8
12. Crewe C, Funcke JB, Li S, et al. Extracellular vesicle-based interorgan transport of mitochondria from energetically stressed adipocytes. Cell Metab 2021;33:1853–1868.e11
13. Cohen MJ, Chirico WJ, Lipke PN. Through the back door: unconventional protein secretion. Cell Surf 2020;6:100045
14. Balmer EA, Faso C. The road less traveled? Unconventional protein secretion at parasite-host interfaces. Front Cell Dev Biol 2021;9:662711
15. Villeneuve J, Bassaganyas L, Lepreux S, et al. Unconventional secretion of FABP4 by endosomes and secretory lysosomes. J Cell Biol 2018;217:649–665
16. Josephrajan A, Hertzel AV, Bohm EK, et al. Unconventional secretion of adipocyte fatty acid binding protein 4 is mediated by autophagic proteins in a sirtuin-1-dependent manner. Diabetes 2019;68:1767–1777
17. Hotamisligil GS, Bernlohr DA. Metabolic functions of FABPs–mechanisms and therapeutic implications. Nat Rev Endocrinol 2015;11:592–605
18. Coe NR, Simpson MA, Bernlohr DA. Targeted disruption of the adipocyte lipid-binding protein (aP2 protein) gene impairs fat cell lipolysis and increases cellular fatty acid levels. J Lipid Res 1999;40:967–972
19. Shum BOV, Rolph MS, Sewell WA. Mechanisms in allergic airway inflammation - lessons from studies in the mouse. Expert Rev Mol Med 2008;10:e15
20. Ghelfi E, Yu CW, Elmasri H, et al. Fatty acid binding protein 4 regulates VEGF-induced airway angiogenesis and inflammation in a transgenic mouse model: implications for asthma. Am J Pathol 2013;182:1425–1433
21. Zeng J, Sauter ER, Li B. FABP4: a new player in obesity-associated breast cancer. Trends Mol Med 2020;26:437–440
22. Najt CP, Khan SA, Heden TD, et al. Lipid droplet-derived monounsaturated fatty acids traffic via PLIN5 to allosterically activate SIRT1. Mol Cell 2020;77:810–824.e8
23. Wang H, Wan X, Pilch PF, Ellisen LW, Fried SK, Liu L. An AMPK-dependent, non-canonical p53 pathway plays a key role in adipocyte metabolic reprogramming. eLife 2020;9:e63665
24. Huang Y, Yong P, Dickey D, Vora SM, Wu H, Bernlohr DA. Inflammasome activation and pyroptosis via a lipid-regulated SIRT1-p53-ASC axis in macrophages from male mice and humans. Endocrinology 2022;163:bqac014.
25. Shen H, Maki CG. Pharmacologic activation of p53 by small-molecule MDM2 antagonists. Curr Pharm Des 2011;17:560–568
26. Wolins NE, Quaynor BK, Skinner JR, et al. OP9 mouse stromal cells rapidly differentiate into adipocytes: characterization of a useful new model of adipogenesis. J Lipid Res 2006;47:450–460
27. Hollstein M, Sidransky D, Vogelstein B, Harris CC. p53 Mutations in human cancers. Science 1991;253:49–53
28. Levine AJ. p53, The cellular gatekeeper for growth and division. Cell 1997;88:323–331
29. Chang BD, Broude EV, Dokmanovic M, et al. A senescence-like phenotype distinguishes tumor cells that undergo terminal proliferation arrest after exposure to anticancer agents. Cancer Res 1999;59:3761–3767
30. Debacq-Chainiaux F, Erusalimsky JD, Campisi J, Toussaint O. Protocols to detect senescence-associated beta-galactosidase (SA-βgal) activity, a biomarker of senescent cells in culture and in vivo. Nat Protoc 2009;4:1798–1806
31. Saul D, Kosinsky RL, Atkinson EJ, et al. A new gene set identifies senescent cells and predicts senescence-associated pathways across tissues. Nat Commun 2022;13:4827
32. Weeda G, Donker I, de Wit J, et al. Disruption of mouse ERCC1 results in a novel repair syndrome with growth failure, nuclear abnormalities and senescence. Curr Biol 1997;7:427–439
33. Niedernhofer LJ, Odijk H, Budzowska M, et al. The structure-specific endonuclease Ercc1-Xpf is required to resolve DNA interstrand cross-link-induced double-strand breaks. Mol Cell Biol 2004;24:5776–5787
34. Lakin ND, Jackson SP. Regulation of p53 in response to DNA damage. Oncogene 1999;18:7644–7655
35. Kim J, Kundu M, Viollet B, Guan KL. AMPK and mTOR regulate autophagy through direct phosphorylation of Ulk1. Nat Cell Biol 2011;13:132–141
36. Saxton RA, Sabatini DM. mTOR Signaling in growth, metabolism, and disease. Cell 2017;168:960–976
37. Hao J, Zhang Y, Yan X, et al. Circulating adipose fatty acid binding protein is a new link underlying obesity-associated breast/mammary tumor development. Cell Metab 2018;28:689–705.e5

38. Guaita-Esteruelas S, Saavedra-García P, Bosquet A, et al. Adipose-derived fatty acid-binding proteins plasma concentrations are increased in breast cancer patients. Oncologist 2017;22:1309–1315
39. Hao J, Yan F, Zhang Y, et al. Expression of adipocyte/macrophage fatty acid-binding protein in tumor-associated macrophages promotes breast cancer progression. Cancer Res 2018;78:2343–2355
40. Koeck ES, Iordanskaia T, Sevilla S, et al. Adipocyte exosomes induce transforming growth factor beta pathway dysregulation in hepatocytes: a novel paradigm for obesity-related liver disease. J Surg Res 2014;192: 268–275
41. Rosina M, Ceci V, Turchi R, et al. Ejection of damaged mitochondria and their removal by macrophages ensure efficient thermogenesis in brown adipose tissue. Cell Metab 2022;34:533–548.e12
42. Kim DE, Dollé MET, Vermeij WP, et al. Deficiency in the DNA repair protein ERCC1 triggers a link between senescence and apoptosis in human fibroblasts and mouse skin. Aging Cell 2020;19:e13072
43. Mindikoglu AL, Abdulsada MM, Jain A, et al. Intermittent fasting from dawn to sunset for four consecutive weeks induces anticancer serum proteome response and improves metabolic syndrome. Sci Rep 2020;10:18341
44. Kang JG, Lago CU, Lee JE, et al. A mouse homolog of a human TP53 germline mutation reveals a lipolytic activity of p53. Cell Rep 2020;30:783–792.e5
45. Laubach K, Zhang J, Chen X. The p53 family: a role in lipid and iron metabolism. Front Cell Dev Biol 2021;9:715974
46. Wu Y, Deng W, Klinke DJ 2nd. Exosomes: improved methods to characterize their morphology, RNA content, and surface protein biomarkers. Analyst (Lond) 2015;140:6631–6642